OPEN

Mapping the Functional Boundaries of the Speech Articulation Network Using Positive and Negative Direct Electrical Stimulation With Resting-State Functional MRI

Lara Maria Viola, MS[‡*], Manuela Moretto, PhD[‡*], Luca Zigiotto, PsyD[§‖§§], Stefano Tambalo, MS[‡¶#], Luciano Annicchiarico, MD[§‖], Martina Venturini, MD[§‖], Jorge Jovicich, PhD[‡], Silvio Sarubbo, MD, PhD[§‖††‡‡**]**

[‡]CIMeC, Center for Mind/Brain Sciences, University of Trento, Rovereto (Trento), Italy; [§]Department of Neurosurgery, "S. Chiara" University-Hospital, Azienda Provinciale per i Servizi Sanitari, Trento, Italy; [‖]Structural and Functional Connectivity Lab, S.Chiara Hospital, APSS Trento, Trento, Italy; [¶]Department of Physics, University of Torino, Torino, Italy; [#]Department of Molecular Biotechnology and Health Sciences, University of Torino, Torino, Italy; [††]Department of Cellular, Computation and Integrative Biology (CIBIO), University of Trento, Trento, Italy [‡‡]Centre for Medical Sciences (CISMED), University of Trento, Trento, Italy; [§§]Department of Psychology, "S. Chiara" University-Hospital, Azienda Provinciale per i Servizi Sanitari, Trento, Italy

*Lara Maria Viola and Manuela Moretto contributed equally to this work and are first authors.

**Jorge Jovicich and Silvio Sarubbo contributed equally to this work and are last authors.

Correspondence: Lara Maria Viola, MS, CIMeC, Center for Mind/Brain Sciences, University of Trento, Piazza della Manifattura 1, Rovereto (TN) 38068, Italy.
Email: laraviola.psicologa@gmail.com

Received, November 21, 2024; **Accepted,** April 21, 2025; **Published Online,** July 25, 2025.

Neurosurgery 00:1–11, 2025

https://doi.org/10.1227/neu.0000000000003613

BACKGROUND AND OBJECTIVES: Resting-state functional MRI (rs-fMRI) is a noninvasive tool for studying brain function, with growing applications in clinical oncology, such as preoperative planning and brain reorganization mapping. Direct electrical stimulation (DES) during awake surgery remains the gold standard for causally identifying functional brain regions. Although previous studies have mapped the speech articulation network (SAN) from rs-fMRI using DES-positive points, the inclusion of DES-negative points remains unexplored. This study integrates both positive and negative DES data to create a more comprehensive SAN atlas and refine its functional borders using presurgical functional connectivity from glioma patients.

METHODS: We analyzed 25 glioma patients (16 high-grade, 9 low-grade) who underwent awake surgery with DES mapping for speech articulation. Seventy-four DES points (32 positive, 42 negative) were identified in gray matter. Presurgical rs-fMRI data were used for seed-based connectivity analysis, with DES-positive and DES-negative points analyzed separately. Group SAN-positive and SAN-negative networks were assessed for overlap across each other and with regions from an anatomical atlas. DES-negative and DES-positive points were used to estimate the sensitivity and specificity of the group SAN-positive network at different thresholds for group frequency.

RESULTS: The DES-positive SAN was bilaterally located in the rolandic operculum, inferior frontal gyrus, and superior temporal gyrus, consistent with previous studies. DES-negative points revealed distinct connectivity patterns, with only partial overlap, helping to delineate the SAN's functional borders, particularly in the central sulcus (posterior and anterior) and inferior frontal gyrus (pars triangularis and opercularis). Anticorrelated networks from DES-positive points further differentiated the roles of positive and negative sites within the SAN. A 41% threshold in the SAN-positive gives approximately 80% specificity and sensitivity.

CONCLUSION: DES-positive points define the SAN robustly. DES-negative points served to establish a threshold for the group SAN atlas and a more detailed definition of the functional SAN borders.

KEY WORDS: Brain surgery, Brain mapping, Direct electrical stimulation, Functional magnetic resonance imaging, Glioma, Presurgical planning, Resting state

ABBREVIATIONS: AAL3, Automated Anatomical Labelling Atlas 3; **AwS,** awake surgery; **DES,** direct electrical stimulation; **HGGs,** high-grade gliomas; **LGGs,** low-grade gliomas; **rs-fMRI,** resting-state fMRI; **SAN,** speech articulation network.

Supplemental digital content is available for this article at neurosurgery-online.com.

Resting-state functional MRI (rs-fMRI) is a powerful technique for exploring the functional organization of the human brain.[1,2] Its emerging clinical applications hold significant potential for clinical practice, particularly in preoperative planning[3-11] and in noninvasive observation of brain reorganization because of disease[12,13] or various therapies.[3,14,15] rs-fMRI is particularly valuable in detecting whole-brain network distributions through seed analysis based on highly specific causal mapping, such as direct electrical stimulation (DES) during awake surgery (AwS).[16]

Among the functions explored with presurgical rs-fMRI, speech articulation is crucial, requiring an understanding of its brain areas for preservation during surgery.[16] The speech articulation network (SAN) is distinct from the classical linguistic network.[17-20] Its bilateral functional connectivity has been confirmed through various techniques and multimodal studies.[16,21,22] Intraoperative mapping further supports this, showing systematic speech arrest in the left or right ventral premotor cortex, independent of language lateralization.[23-25] Therefore, language lateralization was not considered in this study.

In 2018, a seed-based rs-fMRI analysis combined with DES causal mapping was pioneered in a small cohort of glioma patients to map the whole-brain distribution of the speech articulatory functional network, SAN.[16] Furthermore, in 2020, the first integrated and comprehensive probabilistic cortical and subcortical atlas of critical structures mediating human brain functions based on DES data was reported, providing a well-validated tool for exploring cerebral processing and performing safe surgical resections in eloquent areas.[21] This study included a probabilistic SAN atlas derived from 142 DES-positive points for speech articulation. A recent study demonstrated that, in a cohort of high-grade and low-grade glioma (HGGs and LGGs, respectively) patients, the SAN atlas generated from a small sample of just 7 patients,[16] was able to predict the subject-specific SAN with high spatial accuracy (within <1 mm of SAN points identified via DES

TABLE 1. Demographic and Clinical Information of the Study Sample

	Total	LGGs	HGGs
Patients	26	9	17
Sex (#males)	20	7	13
sex (#females)	6	2	4
Handedness (#Left)	1	1	—
Handedness (#Right)	24	7	17
Handedness (#Ambi)	1	1	—
Age (years mean, SD)	45 ± 12	37 ± 14	49 ± 9
Tumor characteristics			
Tumor lateralization (#left)	14	4	10
Tumor lateralization (#right)	12	5	7
Tumor World Health Organization grade (#patients)	—	Grade I (1), Grade II (8)	Grade III (8), Grade IV (9)
Isocitrate dehydrogenase mutation (#patients)	12	5	7
MGMT methylation (#patients)	7	1	6
Tumor location (#frontal)	9	1	8
Tumor location (#frontoinsular/#Insular)	3	1	2
Tumor location (#frontotemporal)	2	—	2
Tumor location (#frontoparietal)	1	—	1
Tumor location (#parietal)	2	1	1
Tumor location (#temporal)	6	4	2
Tumor location (#temporoparietal)	1	—	1
Tumor location (#SMA)	1	1	—

HGGs, high-grade gliomas; LGGs, low-grade gliomas; MGMT, 06-methylguanine-DNA methyltransferase; SMA, supplementary motor area.

TABLE 2. Summary of DES Points (Positive and Negative) Verified to be on Gray Matter

Speech arrest DES points	Total	Left hemisphere	Right hemisphere
Total	74		
Positive	32	14	18
Negative	42	16	26

DES, direct electrical stimulation.
These points were collected during awake surgery while mapping the speech arrest network in the group described in Table 1.

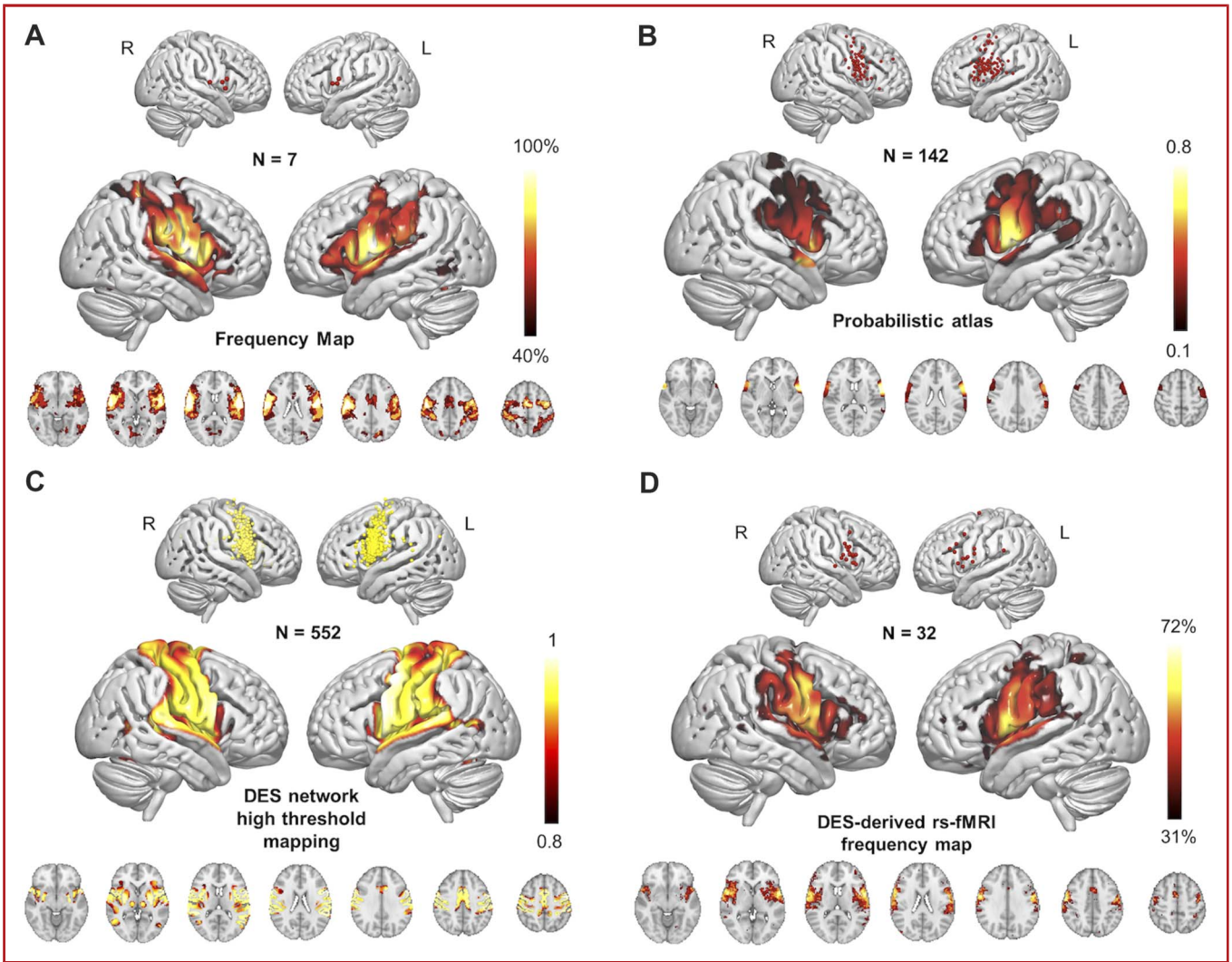

FIGURE 1. *Robustness of the SAN as defined from positive DES sites.* **A**, *Modified from Zacà et al, Human Front Neurosci, 2018: SAN map as the spatial frequency distribution of presurgical resting-state fMRI data from 7 glioma patients using seed-based analysis on 7 DES points (Zacà et al, 2018). Color bar represents % of subjects with common SAN voxel.* **B**, *Modified from Sarubbo et al, Neuroimage 2020: the probability distribution of the cortical responses for speech articulation function (142 DES points, Sarubbo et al, 2020). Color scale reflects the confidence interval of speech articulation function.* **C**, *Modified from Coletta et al, Brain 2024: Integration of cortical DES points (552) derived probabilistic atlas of human brain function from glioma patients with resting-state connectome mapping from 1000 healthy subjects (Coletta et al, 2024).* **D**, *This study: positive DES-derived rs-fMRI frequency map of 25 glioma patients using seed-based analysis (32 DES points). Color bar represents % of DES points with common SAN voxel. All data is shown on the MNI cortical surface and axial slices. DES, direct electrical stimulation; rs-fMRI, resting-state functional MRI; SAN, speech articulation network.*

TABLE 3. Brain Structures Included in the DES-Positive SAN

AAL3 atlas ROIs	% Overlap with DES-positive SAN
Rolandic operculum R	59
Rolandic operculum L	52
Insula R	50
Insula L	49
Superior temporal gyrus L	45
IFG, pars opercularis R	44
IFG, pars opercularis L	42
Heschl gyrus L	36
Heschl gyrus R	35
Supramarginal gyrus L	32
Supramarginal gyrus _R	26
Postcentral gyrus L	25
Supplementary motor area R	23
Precentral gyrus R	23
Supplementary motor area L	21
IFG, pars triangularis R	20
Superior temporal gyrus R	20
Postcentral gyrus R	17
Temporal pole L	17
Posterior orbital gyrus L	16
Putamen L	16
Olfactory cortex L	13
Precentral gyrus L	12
Medial orbital gyrus L	12
Temporal pole R	11
IFG, pars triangularis L	10

AAL3, Automated Anatomical Labelling Atlas 3; DES, direct electrical stimulation; IFG, inferior frontal gyrus; L, left; R, right; ROIs, regions of interest; SAN, speech articulation network. Percent spatial overlap (thresholded by ≥10%) between the DES-positive SAN network (25 glioma patients, 32 DES-positive points) and anatomical cortical regions of the AAL3 Atlas.

during AwS) from presurgical rs-fMRI data.[10] These findings were further supported by a recent multimodal study, which integrated DES data from 612 brain tumor patients undergoing AwS with rs-fMRI data from a large cohort of 1000 healthy subjects spanning 12 functional domains.[26] Despite these advancements, all currently available DES-based atlases share a critical limitation: They have all been constructed from DES-positive functional points while neglecting data from negative points, typically mapped during AwS. Positive points indicate regions where stimulation elicits a specific functional response, whereas negative points show areas where stimulation does not produce the expected response.[27,28] The consideration of both positive and negative points is important for several reasons. Using both pieces of information allows for a better understanding of the true extent and boundaries of functional areas, providing a more comprehensive network definition. In addition, increased specificity and sensitivity would be possible by distinguishing functional regions from nonfunctional ones, reducing false positives and enhancing the reliability of the maps. Better definition of borders between positive and negative functional DES could also help the neurosurgeon during the cortical mapping. In this study, we adopted an innovative approach to map brain networks using a larger data set of causal mapping data derived exclusively from multimodal functional data at the individual level (ie, using patient-specific SAN DES points as seeds on the patient's presurgical rs-fMRI). Importantly, our methodology includes a greater number of negative DES points compared with positive ones. It also incorporates an evaluation of anticorrelated DES-positive networks, often reflecting inhibitory relationships between functional systems, relative to the DES-negative network. If these 2 networks are distinct, it suggests the brain may organize speech articulation across different types of regions with unique functions. If they are just inverse reflections, it may indicate a more cohesive but oppositional system, where 1 set of region "activates" while the other "deactivates" during speech production. The aims of the study were as follows: (1) to create the presurgical SAN with an extended data set based exclusively on patients taking into account both positive and negative DES points, (2) to explore for the first time the borders between positive and negative DES networks, and (3) to assess the sensitivity and specificity of DES data at individual level for the SAN.

METHODS

Participants

This study included 26 consecutive patients with brain gliomas (17 HGGs/9 LGGs; 20 male patients/6 female patients; age 45 ± 12 years). Table 1 provides clinical summary information at the group and individual level, respectively (**Supplemental Digital Content 1** [http://links.lww.com/NEU/E905]). The use of data was approved by the local ethical committee authorization ID A734, and patients provided informed consent. The study was conducted according to the ethical standards of the Declaration of Helsinki.

Intraoperative Functional Mapping

All patients underwent AwS, during which a total of 131 cortical sites were collected with DES (5-mm bipolar probe; 60 Hz; 1 ms; 2-4 mA intensity range across the series) to map speech articulation function. Patient-specific DES coordinates were grouped into 2 domains: positive speech arrest sites and negative speech arrest sites. After intraoperative mapping, the DES coordinates were projected onto a postsurgical T1-

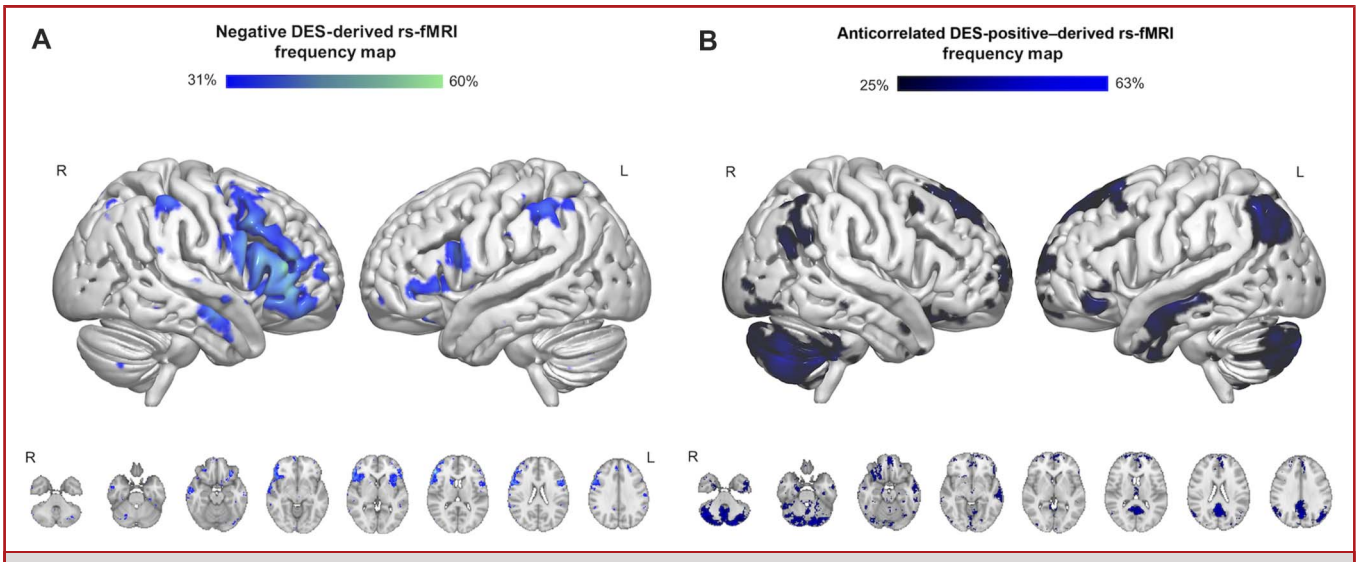

FIGURE 2. *Distinct Speech Articulation Networks: Negative DES points reveal unique connectivity compared with anticorrelated networks from positive DES points.* **A**, *Resting-state fMRI frequency map derived from seed-based analysis using negative DES points (n = 42) as seeds.* **B**, *Functional anticorrelated frequency map showing regions inversely correlated with positive DES points (n = 32), used as seeds for seed-based analysis. Both group frequency networks are shown on the Montreal Neurological Institute 152 brain template. DES, direct electrical stimulation; rs-fMRI, resting-state functional MRI.*

weighted (T1w) image after Gadolinium injection with the same acquisition parameters of the presurgical T1w image. Each DES point underwent visual inspection to confirm its location within the gray matter (these points were retained for the seed-based analysis). Points located at the tumor border or inside the tumor cavity were excluded from the connectivity analysis.

MRI Data Acquisition

Data were acquired with a 1.5 T GE Healthcare MRI scanner. The MRI presurgical acquisition protocol[8,13] included high-resolution T1w image and 12 minutes of rs-fMRI scans (**Supplementa1 Digital Content 1** [http://links.lww.com/NEU/E905]).

Functional Connectivity Analysis

After standard preprocessing of the rs-fMRI data, seed-based connectivity analysis, performed in MATLAB (R2019b), used DES speech arrest sites as regions of interest seeds (**Supplemental Digital Content 1** [http://links.lww.com/NEU/E905]). Distortion by the brain tumor was accounted for during preprocessing, by informing nonlinear warping and resampling to Montreal Neurological Institute space with a lesion binary mask. Goodness of coregistration was carefully assessed by visual inspection. In brief, for each patient, separate functional connectivity maps for DES-positive and DES-negative points were transformed into Montreal Neurological Institute space. Connectivity maps for single subjects were thresholded at z = 0.21, corresponding to a single-voxel *P*-value of .05. To account for multiple comparisons, a false discovery rate correction was applied, maintaining a significance level of $P < .05$. To assess the consistency and variability of SAN-positive and SAN-negative networks across patients, we generated voxel-wise maps of functional connectivity agreement frequency across subjects (**Supplemental Digital Content 1** [http://links.lww.com/NEU/E905]). For example, the group frequency threshold of 41% for the DES-positive network indicates that a voxel belongs to the network if at least 41% of the individual subject-specific seed-based DES-positive networks (ie, 13 of the total 32 networks) show significant functional connectivity in that voxel. The group network anticorrelated from DES-positive points was calculated similarly.

Specificity and Sensitivity of the SAN-Positive Network

Sensitivity and specificity of the SAN-positive network were calculated across different network thresholds using standard definitions (**Supplemental Digital Content 1** [http://links.lww.com/NEU/E905]).

RESULTS

Quality Assurance of DES Points for Seed-Based Analysis

As a result of the quality assurance procedure, a total of 57 DES points (1 DES-positive, 56 DES-negative) were discarded for the seed-based connectivity analysis because of falling inside or at the borders of the tumor mask (**Supplemental Digital Content 2** [http://links.lww.com/NEU/E906] shows some examples of discarded points). The high proportion of DES-negative points within the tumor cavity and along its borders is consistent with tumor-induced damage. This reflects the fact that it is more likely to find positive points outside the tumor than inside, at the cortical level. This is due to the fact that the tumor disrupts eloquent neural pathways in these regions. As a result, stimulation in these areas is less likely to elicit functional responses. Therefore, the analysis included 25 patients instead of 26. Table 2 describes

TABLE 4. Brain Structures Included in the DES-Negative SAN

AAL3 ROIs	% Overlap with DES-negative SAN
IFG, pars opercularis R	46
IFG, pars triangularis R	41
IFG, pars orbitalis R	39
IFG, pars opercularis L	33
Posterior orbital gyrus L	24
IFG, pars triangularis L	21
Middle frontal gyrus R	20
Insula L	20
Inferior parietal gyrus L	17
Lateral orbital gyrus R	17
Precentral gyrus R	17
Insula R	16
Inferior parietal gyrus R	14
Middle temporal gyrus R	13
Anterior orbital gyrus R	13
Supramarginal gyrus R	11
IFG, pars orbitalis L	11
Angular gyrus R	10

Percent spatial overlap (thresholded at ≥10%) between the DES-negative SAN network (25 glioma patients, 42 DES-positive points) and anatomical cortical regions of the AAL3 Atlas. AAL3, Automated Anatomical Labelling Atlas 3; DES, direct electrical stimulation; IFG, inferior frontal gyrus; L, left; R, right; ROIs, regions of interest; SAN, speech articulation network.

the DES points that passed the quality assurance and that were used for the seed-based connectivity analysis.

The SAN From DES-Positive Data

For a visual comparison with previously presented DES-positive SAN atlases, Figure 1 includes atlases from Zacà et al, 2018 (Figure 1A, 7 DES points and rs-fMRI from 7 patients); Sarubbo et al, 2020 (Figure 1B, 142 DES points); and Coletta et al, 2024 (Figure 1C, 552 DES points and rs-fMRI from 1000 healthy subjects). Figure 1D shows the SAN DES-positive network from this study, extended to a larger sample of 25 glioma patients, resulting in 32 DES-positive points. The group frequency map (thresholded at > 31%) shows that the main areas involved in the DES-positive SAN are located bilaterally in the rolandic operculum, inferior frontal gyrus, superior temporal gyrus, inferior parietal lobe (supramarginal gyrus), precentral and postcentral gyrus (Table 3). Overall, Figure 1 shows that the SAN-positive network representations are very similar, despite the fact

TABLE 5. Brain Structures Included in the Anticorrelated DES-Positive SAN

AAL3 ROIs	% Overlap
Vermis 8	89
Vermis 9	83
Cerebellum Crus2 L	62
Cerebellum Crus1 R	52
Cerebellum 9 R	51
Cerebellum Crus2 R	49
Angular gyrus L	49
Cerebellum 9 L	43
Posterior cingulate gyrus L	42
Precuneus L	39
Posterior orbital gyrus R	37
Cerebellum 7b R	35
Superior frontal gyrus, medial orbital L	35
Superior frontal gyrus, medial L	32
Cerebellum Crus1 L	32
Posterior cingulate gyrus R	30
Precuneus_R	26
Cerebellum 8 R	24
Angular gyrus R	24
Vermis 7	22
Ventral tegmental area L	21
Red nucleus R	19
Medial orbital gyrus R	19
Cerebellum 6 R	19
Cerebellum 7b L	18
Gyrus rectus R	16
Olfactory cortex R	16
Calcarine fissure L	16
Vermis 4 5	16
Red nucleus L	16
Superior frontal gyrus R	15
Gyrus rectus L	15
ParaHippocampal gyrus R	15
Inferior occipital gyrus R	15

TABLE 5. Continued.

AAL3 ROIs	% Overlap
Middle temporal gyrus L	14
Superior frontal gyrus, medial orbital R	14
Superior frontal gyrus, medial R	13
Vermis 6	13
Inferior temporal gyrus L	12
Cerebellum 8 L	12
Superior frontal gyrus L	12
Cuneus L	11
IFG, pars orbitalis L	11
Cerebellum 4 5 L	11
Middle cingulate L	11
Cerebellum 6 L	11

AAL3, Automated Anatomical Labelling Atlas 3; DES, direct electrical stimulation; IFG, inferior frontal gyrus; L, left; R, right; ROIs, regions of interest; SAN, speech articulation network. Percent overlap (≥10%) between the anticorrelated DES-positive SAN network (25 glioma patients, 32 DES-positive points) and anatomical cortical regions of the AAL3 Atlas.

of being generated from different sample sizes and different types of data (rs-fMRI patient connectome from patient DES seeds, rs-fMRI healthy connectome from patient DES seeds, probabilistic distribution of DES points).

The SAN From DES-Negative Data

To map functional regions that are not related to speech articulation as causally determined from DES-negative points, we computed a seed-based group frequency map from the 42 DES-negative points (Figure 2A). The Automated Anatomical Labelling Atlas 3 (AAL3) brain regions covered by this SAN-negative network are listed in Table 4. The main areas involved are the right inferior frontal gyrus (pars opercularis, triangularis, and orbitalis), posterior and lateral orbital gyrus, and middle frontal gyrus. For comparison purposes, we also computed the functional regions that are anticorrelated to speech articulation function, by creating a seed-based group frequency map of the significant negative correlations from the 32 DES-positive points (Figure 2B). The AAL3 brain regions covered by this anticorrelated SAN network are listed in Table 5. The main areas involved are the vermis, cerebellum, angular gyrus, and posterior cingulate gyrus bilaterally. From Figure 2 and Tables 4 and 5, it can be seen that these 2 networks, the SAN negative and the anticorrelated SAN, are spatially distinct.

Contrasting Positive and Negative SAN

The distinct spatial connectivity patterns between DES-positive and DES-negative regions within the SAN are shown in Figure 3. Despite the close spatial proximity of positive (red) and negative (blue) DES points, as seen in the upper row, their underlying spatial connectivity profiles diverge significantly, as depicted in the lower row. DES-positive and DES-negative points show distinct network connectivity profiles that only partially overlap, indicating that even adjacent points can contribute differently to speech articulation. This contrast underscores the complexity and, at the same time, the specificity of neural organization within the SAN, revealing how closely situated DES points can nonetheless participate in separate and specialized pathways, reflecting the roles of specific brain areas in speech processing.

The DES-negative points were analyzed to further assess the specificity and sensitivity of the SAN+ network. Table 6 reports the true and false positives and negatives at different network thresholds, and Figure 4 shows the resulting changes of sensitivity (blue) and specificity (orange) of the group SAN+ at these thresholds. As expected, increasing the SAN+ network threshold reduces gradually its spatial extent (Figure 4 shows a few examples of the left-hemisphere network at different thresholds). These changes in spatial extent have 2 main effects: (1) At higher thresholds (smaller network extent), the percentage of DES-negative points outside the network increases, indicating higher specificity, and (2) at lower thresholds (larger network extent), the percentage of DES-positive points inside the network increases, indicating higher sensitivity. The sensitivity and specificity profiles show opposite trends as the SAN+ threshold increases, with a crossing around 41% (Figure 4). We found that above the SAN+ threshold of 41%, the sensitivity starts to decrease from 77% and the specificity gradually increases from a value of 85%. This suggests that this threshold of the SAN+ is a good compromise, as larger ones will decrease sensitivity and smaller ones will decrease specificity.

DISCUSSION

This study provides a more comprehensive mapping of the SAN by incorporating both DES-positive and DES-negative points, a novel approach not previously explored. Consistent with previous research,[16,21,26] the DES-positive SAN was robustly identified in bilateral regions such as the rolandic operculum, inferior frontal gyrus, and superior temporal gyrus. We speculate that the bi-hemispheric distribution of the SAN is not related to language lateralization for 2 main reasons. First, we consistently elicited speech arrest functional responses at DES sites in the right hemisphere, despite patients' handedness. All right-handed patients in our group with right-hemisphere tumors (n = 12) underwent DES in the right hemisphere. During surgery, they exhibited speech articulation impairments but showed no language production errors when DES was applied during AwS, consistent with the typical localization of this function in the left hemisphere. Second, we found bi-hemispheric functional connectivity distributions when seeding from DES-positive points, regardless of their hemispheric location. Importantly, the addition of DES-negative points allowed us to delineate the functional

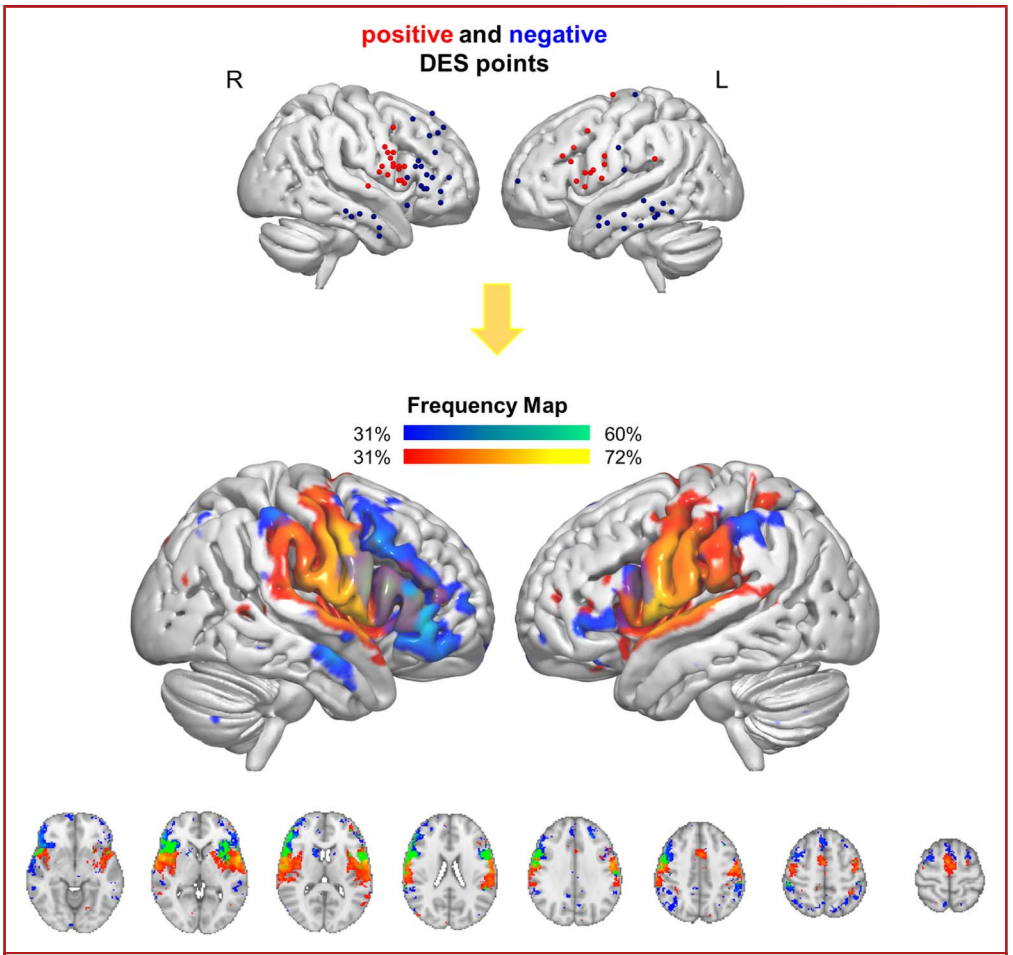

FIGURE 3. *Contrasting DES-positive and negative points in the SANs. The top panel shows the spatial proximity between 32 DES-positive (red) and 42 DES-negative (blue) SAN points. The middle panel reveals distinct functional connectivity patterns derived from these points, with only partial overlap (green) shown in the bottom panel. The 2 group frequency maps are thresholded at the same percentage of number of seed-based points from the total (31%). DES, direct electrical stimulation; SAN, speech articulation network.*

boundaries of the SAN with an unprecedented level of accuracy and particularly within the precentral sulcus and inferior frontal gyrus. Moreover, a threshold of 41% in the DES-positive SAN yielded high sensitivity (~80%) and specificity (~80%), suggesting this threshold as a suitable balance for clinical applications. This is a further result providing a reliable criterion, in the field of functional atlases, to set a threshold with high level of both sensitivity and specificity.

Preoperative Speech Articulation Mapping From DES-Positive Points is Robust

We extended the estimation of the SAN using 1.5 T rs-fMRI data seeded on DES-positive points from 25 glioma patients. The results align qualitatively with previous SAN atlases derived from smaller samples,[16] probabilistic distributions of DES-positive data,[21] and larger data sets with over 500 DES-positive points seeded on 3 T rs-fMRI from 1000 healthy volunteers.[26] On one hand, and despite significant differences in sample sizes, pathologies, and experimental methodologies, the topology of the SAN remains consistent across studies, suggesting the robustness of seed-based rs-fMRI analyses on preoperative data. On the other hand, this consistency highlights, once again, the power regarding reliability of DES-positive points in mapping and identifying the real critical speech articulation regions across different cohorts, methodologies, and in different centers.

Speech Articulation Functional Borders Defined From DES-Negative Points

By considering DES-negative areas during AwS speech articulation mapping, we identified the connected network where stimulation fails to elicit a response. This novel dual mapping

TABLE 6. Data Used to Estimate Sensitivity and Specificity of the SAN-Positive Network

SAN positive thresholds %	TP	TN	FN	FP
25	26	47	4	42
28	25	49	5	40
31	24	57	6	32
34	24	62	6	27
38	23	70	7	19
41	23	76	7	13
44	21	78	9	11
47	21	79	9	10
50	18	80	12	9
53	16	82	14	7
56	11	82	19	7
59	7	82	23	7

DES, direct electrical stimulation; FN, false negatives (DES-positive points outside SAN-positive network); FP, false positives (DES-negative points within the SAN-positive network); IFG, inferior frontal gyrus; L, left; R, right; ROIs, regions of interest; SAN, speech articulation network; TN, true negatives (DES-negative points outside SAN-positive network); TP, true positives (DES-positive points within the SAN-positive network).
The total number of DES points used were 119 (30 positive DES and 89 negative DES).

approach allowed us to differentiate functional from nonfunctional areas more accurately. For the first time, we precisely identified the functional boundaries between these networks using positive and negative causal mappings. Despite the proximity of DES points, the DES-negative and DES-positive networks were spatially distinct, with minimal overlap. We consider this overlap a functional border, including the precentral sulcus and inferior frontal gyrus. This minimal overlap enhances understanding of SAN+ boundaries *without* altering the SAN network defined by DES-positive points, supporting the importance of defining networks from DES-positive points.

As expected, the choice of SAN network threshold affects its spatial extent. The threshold represents the minimum percentage of DES-positive points required to generate seed-based functional connectivity in a given voxel. To determine the optimal threshold for presurgical SAN mapping, we assessed the sensitivity and specificity of the network by comparing the locations of DES-positive and DES-negative points across various thresholds. Our analysis revealed that a 41% group frequency threshold in the DES-positive SAN offers an ideal balance, achieving approximately 80% sensitivity and specificity, thus providing a valuable reference for clinical use. In fact, our examination of the SAN-negative network and the anticorrelated SAN offers novel insights into the broader landscape of speech-articulatory network interconnection in the language and motor frameworks. The SAN-negative network seemed to have a more lateralized pattern compared with the bilateral DES-positive SAN. The fact that the SAN-negative network differs from both the SAN-positive and its anticorrelated network suggests it may involve nonessential or redundant pathways, or regions involved in higher order functions or compensation that do not directly contribute to speech arrest.

Clinical Implications

The overlap between DES-positive and DES-negative areas suggests transitional zones within the speech network rather than core regions for articulation. Although they may not consistently disrupt speech during DES, their role varies individually, highlighting the need for careful mapping. Presurgical definition of the SAN functional borders has key clinical implications. In AwS with DES, it enables precise targeting of critical regions, reducing irrelevant stimulation, mapping time, and improving confidence in avoiding critical areas. In asleep surgery, it enhances preoperative planning and identification of key regions, potentially reducing postoperative language and speech deficits. Overall, clearer functional borders improve intraoperative decision making in AwS and enhance safety and efficacy in asleep surgery.

Limitations

This study advances our understanding of the SAN's functional boundaries, but several limitations exist. With a cohort of 25 glioma patients (HGGs and LGGs), the functional borders may not be fully defined. Larger, more homogeneous samples with both DES-positive and DES-negative data will refine spatial definitions. In addition, variability in AwS protocols and stimulation parameters across centers may affect DES results and SAN mapping accuracy. Brain shift was not explicitly modeled, but factors such as neurosurgeon-verified preoperative/postoperative T1 registrations, cortical-only points, and prior validation[8,10] of presurgical rs-fMRI and DES agreement (<5 mm) suggest minimal impact. Future studies could improve this with intraoperative imaging or brain shift modeling. Neurovascular decoupling may affect blood oxygenation level dependent (BOLD) signals in tumor patients,[29,30] but strong agreement (<5 mm) between presurgical rs-fMRI and awake DES mapping[8,10] supports its reliability. Future studies should address neurovascular decoupling using calibrated fMRI, alternative imaging (eg, arterial spin labeling), or cerebrovascular reactivity.[31] Our speech articulation maps include low-grade (n = 9) and high-grade (n = 17) glioma patients. While lower grade cases may show differences, studies suggest limited plasticity in this network.[26,32] DES during AwS ensures functional validation. Future studies could investigate reorganization with longitudinal or advanced tracking methods. This study used a 1.5 T MRI, which has lower BOLD specificity than higher field systems. Future studies should use 3 T MRI for improved precision and validation.

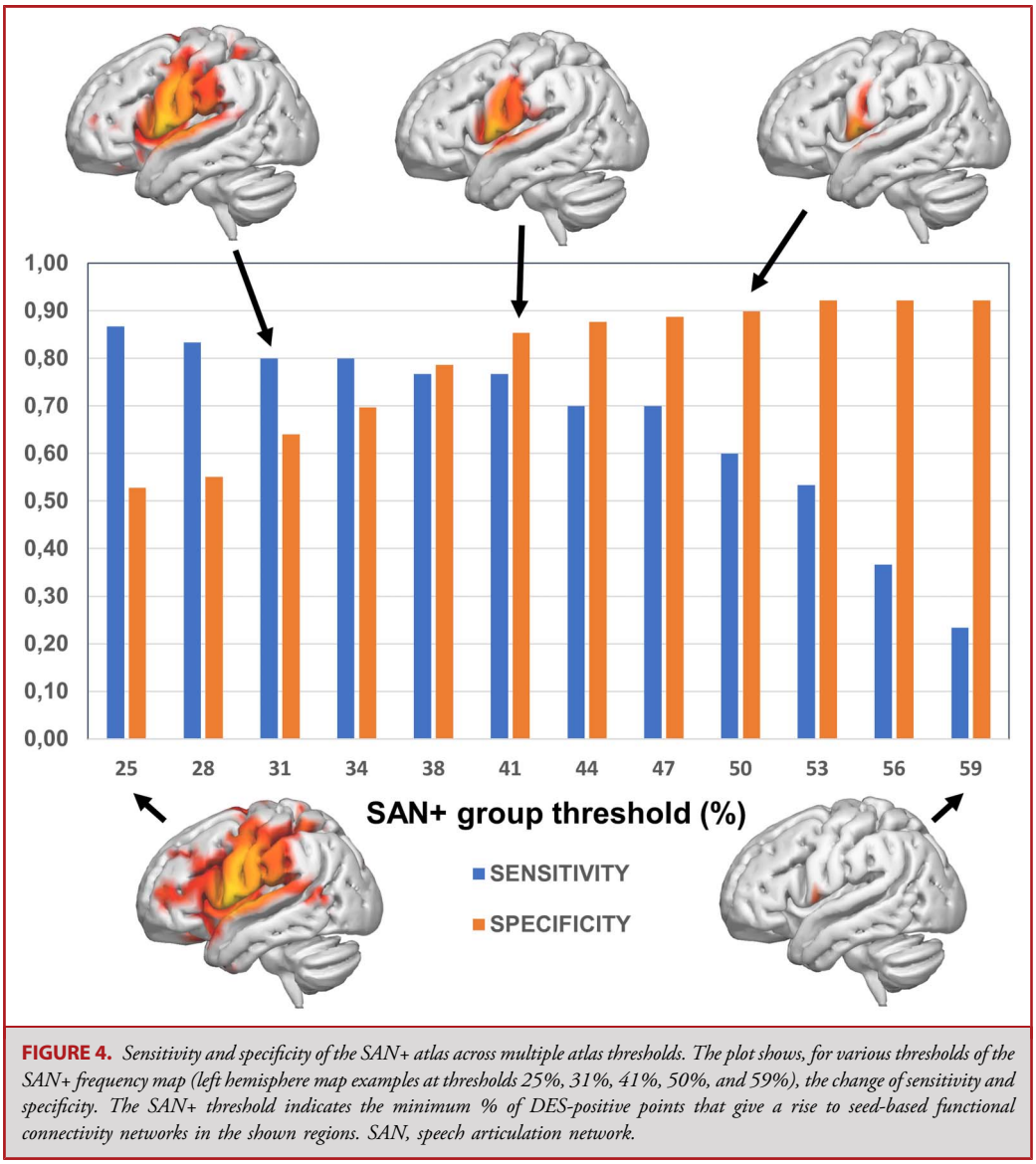

FIGURE 4. *Sensitivity and specificity of the SAN+ atlas across multiple atlas thresholds. The plot shows, for various thresholds of the SAN+ frequency map (left hemisphere map examples at thresholds 25%, 31%, 41%, 50%, and 59%), the change of sensitivity and specificity. The SAN+ threshold indicates the minimum % of DES-positive points that give a rise to seed-based functional connectivity networks in the shown regions. SAN, speech articulation network.*

CONCLUSION

This study represents a significant step forward in the use of DES-negative data to improve the definition of functional brain networks, particularly in the context of mapping the SAN. Incorporating both DES-positive and DES-negative points provides a more precise and clinically relevant map for preoperative planning, which is expected to help improve the effectiveness of neurosurgical interventions. Further efforts should be performed to investigate how these findings can be more and more applied across different neurological and neurosurgical contexts. To support the potential use of these results in presurgical planning and future studies exploring the SAN with various neuroimaging techniques, we provide spatial frequency maps of the SAN based on DES-positive and DES-negative points (https://neurovault.org/).

Funding

This project was supported by Hub Life Science- Advanced Diagnosis (HLS-AD), PNRR PNC-E3-2022-23683266 PNC-HLS-DA, INNOVA – CUP: E63C22003780001», funded by the Italian Ministry of Health under the National Complementary Plan Innovative Health Ecosystem - Unique Investment Code: PNC-E.3.

Disclosures

The authors have no personal, financial, or institutional interest in any of the drugs, materials, or devices described in this article.

REFERENCES

1. Ng S, Deverdun J, Lemaitre AL, et al. Precuneal gliomas promote behaviorally relevant remodeling of the functional connectome. *J Neurosurg.* 2023;138(6):1531-1541.
2. Mandal AS, Brem S, Suckling J. Brain network mapping and glioma pathophysiology. *Brain Commun.* 2023;5(2):fcad040.
3. Lee MH, Smyser CD, Shimony JS. Resting-state fMRI: a review of methods and clinical applications. *AJNR Am J Neuroradiol.* 2013;34(10):1866-1872.
4. Duffau H, Capelle L, Denvil D, et al. Usefulness of intraoperative electrical subcortical mapping during surgery for low-grade gliomas located within eloquent brain regions: functional results in a consecutive series of 103 patients. *J Neurosurg.* 2003;98(4):764-778.
5. Duffau H, Lopes M, Arthuis F, et al. Contribution of intraoperative electrical stimulations in surgery of low grade gliomas: a comparative study between two series without (1985-96) and with (1996-2003) functional mapping in the same institution. *J Neurol Neurosurg Psychiatry.* 2005;76(6):845-851.
6. Bizzi A, Blasi V, Falini A, et al. Presurgical functional MR imaging of language and motor functions: validation with intraoperative electrocortical mapping. *Radiology.* 2008;248(2):579-589.
7. Rosazza C, Zacà D, Bruzzone MG. Pre-surgical brain mapping: to rest or not to rest? *Front Neurol.* 2018;9:520.
8. Zacà D, Jovicich J, Corsini F, Rozzanigo U, Chioffi F, Sarubbo S. ReStNeuMap: a tool for automatic extraction of resting-state functional MRI networks in neurosurgical practice. *J Neurosurg.* 2019;131(3):764-771.
9. Luna LP, Sherbaf FG, Sair HI, Mukherjee D, Oliveira IB, Köhler CA. Can preoperative mapping with functional MRI reduce morbidity in brain tumor resection? A systematic review and meta-analysis of 68 observational studies. *Radiology.* 2021;300(2):338-349.
10. Moretto M, Luciani BF, Zigiotto L, et al. Resting state functional networks in gliomas: validation with direct electric stimulation using a new tool for planning brain resections. *Neurosurgery.* 2024;95(6):1358-1368.
11. Maesawa S, Bagarinao E, Fujii M, et al. Evaluation of resting state networks in patients with gliomas: connectivity changes in the unaffected side and its relation to cognitive function. *PLoS One.* 2015;10(2):e0118072.
12. Ghinda DC, Wu JS, Duncan NW, Northoff G. How much is enough-Can resting state fMRI provide a demarcation for neurosurgical resection in glioma? *Neurosci Biobehav Rev.* 2018;84:245-261.
13. Saviola F, Zigiotto L, Novello L, et al. The role of the default mode network in longitudinal functional brain reorganization of brain gliomas. *Brain Struct Funct.* 2022;227(9):2923-2937.
14. Boerwinkle VL, Sussman BL, Wyckoff SN, et al. Discerning seizure-onset v. propagation Zone: pre-and-post-operative resting-state fMRI directionality and Boerwinkle Neuroplasticity Index. *NeuroImage Clin.* 2022;35:103063.
15. Struckmann W, Bodén R, Gingnell M, Fällmar D, Persson J. Modulation of dorsolateral prefrontal cortex functional connectivity after intermittent theta-burst stimulation in depression: combining findings from fNIRS and fMRI. *NeuroImage Clin.* 2022;34:103028.
16. Zacà D, Corsini F, Rozzanigo U, et al. Whole-brain network connectivity underlying the human speech articulation as emerged integrating direct electric stimulation, resting state fMRI and tractography. *Front Hum Neurosci.* 2018;12:405.
17. Guenther FH, Hickok G. Chapter 58 - Neural models of motor speech control. In: Hickok G Small SL, eds. *Neurobiology of Language*. Academic Press; 2016:725-740.
18. Lu J, Zhao Z, Zhang J, et al. Functional maps of direct electrical stimulation-induced speech arrest and anomia: a multicentre retrospective study. *Brain J Neurol.* 2021;144(8):2541-2553.
19. Nakai Y, Jeong JW, Brown EC, et al. Three- and four-dimensional mapping of speech and language in patients with epilepsy. *Brain A J Neurol.* 2017;140(5):1351-1370.
20. Hsu CW, Huang CC, Hsu CCH, Bi Y, Tzeng OJL, Lin CP. Revisiting human language and speech production network: a meta-analytic connectivity modeling study. *NeuroImage.* 2025;306:121008.
21. Sarubbo S, Tate M, De Benedictis A, et al. Mapping critical cortical hubs and white matter pathways by direct electrical stimulation: an original functional atlas of the human brain. *NeuroImage*. 2020;205:116237.
22. Könönen M, Tamsi N, Säisänen L, et al. Non-invasive mapping of bilateral motor speech areas using navigated transcranial magnetic stimulation and functional magnetic resonance imaging. *J Neurosci Methods.* 2015;248:32-40.
23. Mayka MA, Corcos DM, Leurgans SE, Vaillancourt DE. Three-dimensional locations and boundaries of motor and premotor cortices as defined by functional brain imaging: a meta-analysis. *NeuroImage.* 2006;31(4):1453-1474.
24. Chang EF, Raygor KP, Berger MS. Contemporary model of language organization: an overview for neurosurgeons. *J Neurosurg.* 2015;122(2):250-261.
25. Tate MC, Herbet G, Moritz-Gasser S, Tate JE, Duffau H. Probabilistic map of critical functional regions of the human cerebral cortex: Broca's area revisited. *Brain J Neurol.* 2014;137(Pt 10):2773-2782.
26. Coletta L, Avesani P, Zigiotto L, et al. Integrating direct electrical brain stimulation with the human connectome. *Brain J Neurol.* 2024;147(3):1100-1111.
27. Mandonnet E, Sarubbo S, Duffau H. Proposal of an optimized strategy for intraoperative testing of speech and language during awake mapping. *Neurosurg Rev.* 2017;40(1):29-35.
28. Sanai N, Mirzadeh Z, Berger MS. Functional outcome after language mapping for glioma resection. *N Engl J Med.* 2008;358(1):18-27.
29. Zacà D, Jovicich J, Nadar SR, Voyvodic JT, Pillai JJ. Cerebrovascular reactivity mapping in patients with low grade gliomas undergoing presurgical sensorimotor mapping with BOLD fMRI. *J Magn Reson Imaging.* 2014;40(2):383-390.
30. Agarwal S, Sair HI, Pillai JJ. The problem of neurovascular uncoupling. *Neuroimaging Clin N Am.* 2021;31(1):53-67.
31. Agarwal S, Welker KM, Black DF, et al. Detection and mitigation of neurovascular uncoupling in brain gliomas. *Cancers.* 2023;15(18):4473.
32. van Geemen K, Herbet G, Moritz-Gasser S, Duffau H. Limited plastic potential of the left ventral premotor cortex in speech articulation: evidence from intraoperative awake mapping in glioma patients. *Hum Brain Mapp.* 2013;35(4):1587.

Acknowledgments

Author contributions: Conceptualization: J.J. and S.S.; Data collection: L.Z., L.A., M.V., S.S.; Methodology: L.M.V., M.M., S.T. and J.J.; Software: L.M.V., M.M., S.T.; Data Analysis: L.M.V., M.M.; Visualization: L.M.V., M.M., L.Z.; Supervision: J.J. and S.S.; Writing Original Draft: L.M.V. and J.J.; All authors reviewed the manuscript.

Supplemental digital content *is available for this article at neurosurgery-online.com.*

Supplemental Digital Content 1. **Text**. Participants. MRI data acquisition. Resting-state fMRI preprocessing. Seed-based connectivity analysis. Specificity and sensitivity of the SAN-positive network.

Supplemental Digital Content 2. **Figure**. Example of discarded DES points. The crosshairs indicate DES point locations. **A**, DES point falling within the tumor cavity. **B**, DES points falling within the tumor cavity. **C**, DES point located at the tumor border. **D**, DES point located at the tumor border.